Multiwavelength Magnetic-Free Optical Isolator by Optical Pumping in Warm Atoms

Yiqi Hu,[1,2] Shicheng Zhang,[1] Yihong Qi,[1] Gongwei Lin,[1,*] Yueping Niu,[1,3,†] and Shangqing Gong[1,3,‡]

[1] *Department of Physics, East China University of Science and Technology, Shanghai 200237, China*
[2] *School of Materials Science and Engineering, East China University of Science and Technology, Shanghai 200237, China*
[3] *Shanghai Engineering Research Center of Hierarchical Nanomaterials, Shanghai 200237, China*

(Received 19 July 2019; revised manuscript received 26 September 2019; published 4 November 2019)

Realization of magnetic-free nonreciprocal transmission for two or more wavelengths simultaneously is in great demand for multiwavelength optical communication and signal processing. Here, making use of optical pumping, we propose and experimentally demonstrate a magnetic-free multiwavelength isolator based on warm V-type atoms with the assistance of the Doppler effect. Applying ^{85}Rb atoms, isolation ratios of 25 and 28 dB are obtained simultaneously for signal fields at 795 and 780 nm with transmissions higher than 0.85. This work provides an effective way to realize a multiwavelength optical isolator for optical information processing applications.

DOI: 10.1103/PhysRevApplied.12.054004

I. INTRODUCTION

Optical isolators controlling the unidirectional transmission of light are the primary components in optical information processing. Their realization relies on the breaking of the Lorenz reciprocity [1,2]. To date, the most common approach to achieve nonreciprocity is based on the Faraday effect, where bulk magneto-optical crystals are applied. But facing the challenge of miniaturization, a series of new schemes have been proposed to realize magnetic-free nonreciprocity, including the use of the nonlinear effect [3–8], spatiotemporal modulation of permittivity [9–13], optomechanical interaction [14–20], fast-spinning resonators [21], moving Bragg lattices [22,23], the chiral quantum regime [24–28], and the electromagnetically induced transparency of warm atoms [29–31].

Recently, several strategies for magnetic-free tunable isolators have been pursued at different wavelengths by adjusting system parameters [32–35]. For example, the tunable schemes can be realized by adjusting the parameters of the external laser in the linear interband Brillouin scattering system [32] or chiral quantum system [33], changing the input power in the Fano interference system [34], and tuning the coupling strength between mechanical oscillators in an optomechanical system [35]. However, if two or more signals of different wavelengths are incident into the system simultaneously, these tunable isolators only work for one of the signals. Therefore, an investigation of a multiwavelength optical isolator, which can simultaneously work for multiple signals of different wavelengths, should be interesting.

As an important simple method in the field of atomic optics, optical pumping [36] is used to upset the balance of population in different atomic levels and plays crucial roles in laser cooling and trapping [37–39], Bose-Einstein condensation [40,41], precision measurement [42,43], and so on. In our scheme, mature optical pumping technology is used to realize multiwavelength nonreciprocal transmission with the assistance of the Doppler effect. We use optical pumping to induce an asymmetric distribution of the ground-state atoms over the velocity, which can simultaneously transmit or isolate multiple signal fields dependent on their propagating direction. This dynamics supports simultaneous nonreciprocal transmission for two or more signal fields with only one pump field, which can be used to realize a multiwavelength magnetic-free optical isolator. In our proof-of-concept experiment, we demonstrate simultaneous nonreciprocal transmission for two signal fields of different wavelengths (780 and 795 nm) with more than 25 dB of isolation in warm ^{85}Rb atoms. This scheme may have advantages in decreasing the number of optical isolators, and thus it can reduce the complexity of the integrated multiwavelength optical system, such as wavelength division multiplexing (WDM), which can simultaneously transmit two or more optical signals of different wavelengths in the same waveguide.

*gwlin@ecust.edu.cn
†niuyp@ecust.edu.cn
‡sqgong@ecust.edu.cn

The paper is organized as follows. In Sec. II, we illustrate how the optical pumping can lead to simultaneous nonreciprocal transmission for multiple signals of different wavelengths assisted by the Doppler effect. Next, in Sec. III, we design a proof-of-concept experiment and discuss its results. Our conclusions are given in Sec. IV.

II. PRINCIPLE OF OPERATION

The key element of the isolator based on optical pumping is shown in Fig. 1. We first introduce only one signal field to illustrate the physical mechanism. A weak signal field passes through the atomic ensemble from opposite directions along the z axis [Fig. 1(a)]. It couples the transition $|g_1\rangle \rightarrow |e\rangle$ with a detuning $\delta_s = \omega_s - \omega_{g_1e}$, where ω_s is the signal field frequency and ω_{g_1e} is the frequency difference between levels $|g_1\rangle$ and $|e\rangle$ [Fig. 1(b)]. Here, we account only for the longitudinal Doppler effect along the laser beam direction. Because of the Doppler effect, the forward signal field (wave vector k_s, $+z$) is resonantly absorbed by a group of atoms with velocity $v = \delta_s/k_s$, while the backward signal field (wave vector $-k_s$, $-z$) is resonantly absorbed by another group of atoms with velocity $v' = \delta_s/(-k_s) = -v$ [Fig. 1(c)]. Because the atomic velocity satisfies the Maxwell-Boltzmann distribution, the numbers of atoms in the velocity groups v and $-v$ are the same. Therefore, the absorption of the atomic system for the forward and backward signal fields is reciprocal. Nevertheless, if we can create an asymmetrical distribution for the number of atoms in the groups v and $-v$, it is possible to realize nonreciprocal transmission for the forward and backward signal fields. In order to achieve such a goal, a strong pump field propagating in the forward direction (wave vector k_p, $+z$) coupling the transition $|g_1\rangle \rightarrow |f\rangle$ with a detuning $\delta_p = \omega_p - \omega_{g_1f}$ is applied, where ω_p is the pump field frequency and ω_{g_1f} is the frequency difference between levels $|g_1\rangle$ and $|f\rangle$ [Figs. 1(a) and 1(b)]. When the condition $\delta_p = k_p v$ is met, namely, its effective detuning $\delta_p' = \delta_p - k_p v = 0$, the pump field resonates with the group of atoms with velocity v. Then, the absorption and spontaneous emission cycle $|g_1\rangle \rightarrow |f\rangle \rightarrow |g_2\rangle$ happens and leads to a population transfer from the ground state $|g_1\rangle$ to the other one $|g_2\rangle$ [Fig. 1(b)]. Thus, the ground state $|g_1\rangle$ of the atoms with v is emptied, leading to a high transmission for the forward signal field around the position $\delta_s = \delta_p k_s/k_p$. By contrast, the pump field "seen" by the atoms with the velocity $-v$ has an effective detuning $\delta_p' = \delta_p - k_p(-v) = 2\delta_p$, which is far from resonance. It can hardly pump the $-v$ atoms away from the ground state $|g_1\rangle$ and therefore the backward signal field is still absorbed strongly around the position $\delta_s = \delta_p k_s/k_p$. This velocity selective optical pumping thus leads to the nonreciprocal transmission of the signal field, and then it can be used for the optical isolator.

Next, we take the multiple signal fields $\mathbf{k}_{si}$ $(i = 1, 2, 3, \ldots)$ into account. They couple with the ground state $|g_1\rangle$ and different excited states $|e_i\rangle$ with respective frequency detuning δ_{si} in the multilevel atomic system [Fig. 1(d)]. Without the pump field, for the forward case, as long as δ_{si} satisfies $\delta_{si} = k_{si}v$, the multiple signal fields are absorbed by the same atomic group v. Similarly, when these signal fields propagate backward $(-k_{si})$, they are all absorbed by the atomic group $-v$. Exactly as addressed above, when a forward-propagating strong pump field with $\delta_p = k_p v$ is applied, the atomic group v in the ground state $|g_1\rangle$ is emptied, and thus all signal fields satisfying $\delta_{si} = k_{si}v$ inevitably have high transmissions around the position

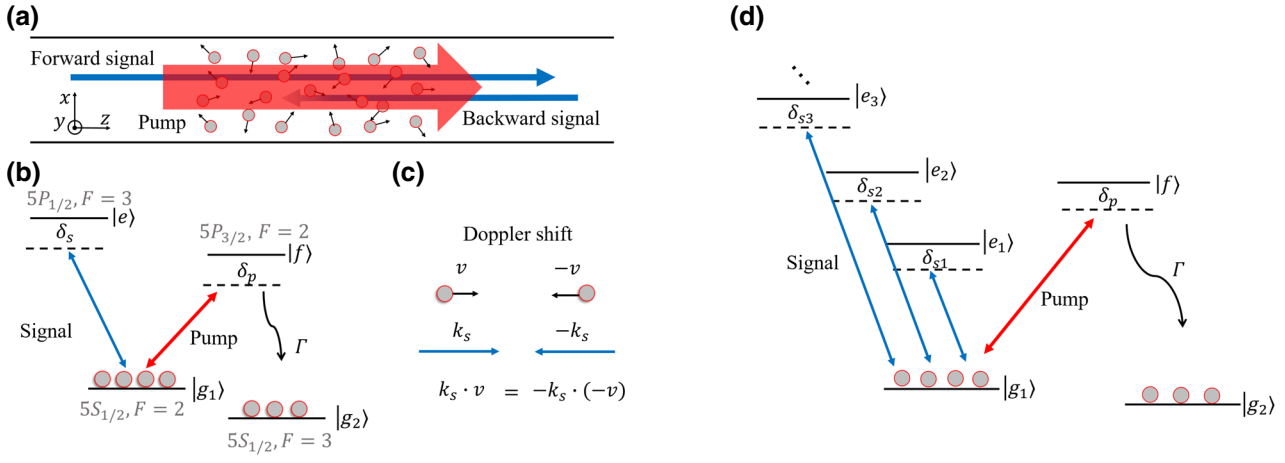

FIG. 1. (a) Schematic illustration of the optical isolator with optical pumping in warm atoms. The forward signal passes through the atoms while the backward signal is absorbed by atoms. (b) V-type level structure used to create nonreciprocity for a signal field. The weak signal and strong pump fields couple to the transition $|g_1\rangle \rightarrow |e\rangle$ and $|g_1\rangle \rightarrow |f\rangle$, with detuning δ_s and δ_p, respectively. (c) The Doppler shifts for the forward and backward signal fields. (d) The multilevel V-type system used to create nonreciprocity for multiple signal fields.

$\delta_{si} = \delta_p k_{si}/k_p$. This leads to the simultaneous nonreciprocal transmission for multiple signal fields around $\delta_{si} = \delta_p k_{si}/k_p$. In a similar way, around $\delta_{si} = -\delta_p k_{si}/k_p$, there is the other nonreciprocal transmission channel, where the backward signals are transmitted and the forward signals are isolated. Take the rubidium (Rb) atoms for an example. If we choose a pump field near 780 nm, the nonreciprocal transmission can be formed simultaneously for the signals at 795 nm ($5S_{1/2} \rightarrow 5P_{1/2}$), 780 nm ($5S_{1/2} \rightarrow 5P_{3/2}$), 421 nm ($5S_{1/2} \rightarrow 6P_{1/2}$), etc. Therefore, in a multiwavelength optical system, such an optical isolator can be used instead of multiple isolators, thus facilitating efficient integration.

III. EXPERIMENT AND DISCUSSION

The proof-of-concept experiment demonstrating multiwavelength isolation is performed with warm ^{85}Rb atoms in a vapor cell 7.5 cm in length. The Rb cell is wrapped in μ-metal for magnetic shielding and a heater coil for controlling atomic density. In our experiment, we keep the atomic temperature to be 70°C. The pump field near 780 nm couples $|5S_{1/2}, F = 2\rangle (|g_1\rangle) \rightarrow |5P_{3/2}, F = 2\rangle (|f\rangle)$. First, we demonstrate the nonreciprocal transmission for a single signal field of 795 nm. The signal field scans near the $|5S_{1/2}, F = 2\rangle (|g_1\rangle) \rightarrow |5P_{1/2}, F = 3\rangle (|e\rangle)$ transition and is divided into two beams incident from the opposite directions $\pm z$ into the cell. In our experiment, the radii of the pump and signal fields are estimated to be 0.9 and 0.7 mm, respectively. The polarizations of the pump and signal fields are orthogonal to each other and can be separated by a polarized beam splitter (PBS). The forward and backward signal fields have the same power of 3 μW. All the transmission spectra are directly measured with the simultaneous presence of the signal fields from both directions.

Without the pump field, both signal fields from opposite directions are almost completely absorbed and their transmissions show good reciprocity, as displayed in Fig. 2(a). Then, we turn on the pump field. The detuning is set to be $2\pi \times 185$ MHz according to our theoretical simulation (see Appendix B). As expected, nonreciprocal transmission spectra of forward (dashed blue line) and backward (solid red line) signals present as shown in Fig. 2(b). Because of $k_s \approx k_p$, the signal field exhibits nonreciprocal transmission at the detuning position of $\delta_s/2\pi = \delta_p/2\pi = 185$ MHz. According to our theoretical analysis, there is also a reversed nonreciprocal channel at $\delta_s/2\pi = -\delta_p/2\pi = -185$ MHz. However, because of the existence of a lower hyperfine excited state $|5P_{1/2}, F = 2\rangle$ in our actual experiment, the signal field around $\delta_s/2\pi = -185$ MHz is near-resonant to this excited state and is absorbed strongly. As a result, we record a lower transmission at $\delta_s/2\pi = -185$ MHz and a higher transmission at $\delta_s/2\pi = 185$ MHz in our experiment. Since transmission is a very important factor for an isolator, we demonstrate the high transmission at $\delta_s/2\pi = 185$ MHz as the isolator performance here. Moreover, we measured the forward and backward transmission at $\delta_s/2\pi = 185$ MHz versus the pump field power, ranging from 1 to 14 mW. As shown in Fig. 2(e), the backward transmission remains nearly zero, while the forward transmission increases from 0.19 to 0.88. In our experiment, the experimental results are very stable and therefore represented by the average value without error bars.

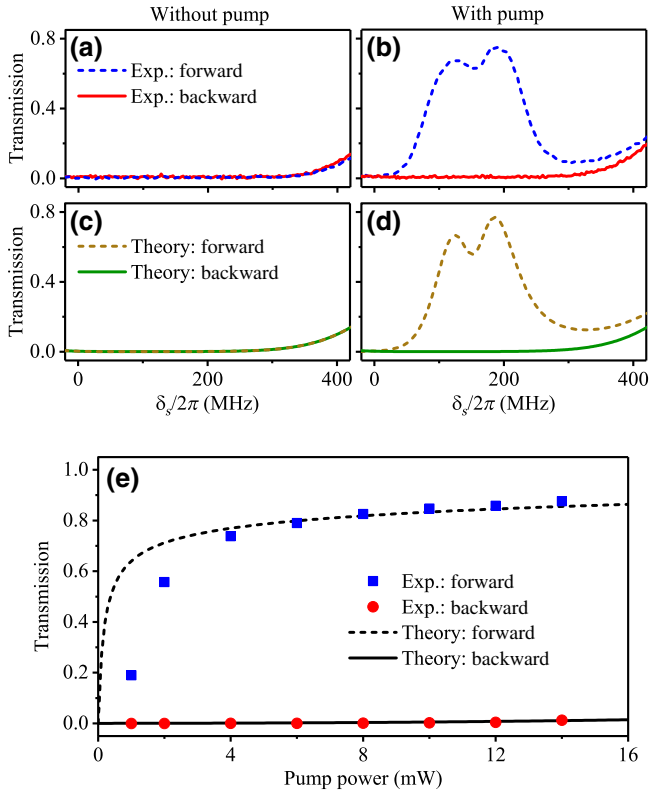

FIG. 2. (a),(b) Experimental observation of normalized transmission versus the detuning of the signal field without and with optical pumping. The pump power is fixed at 4 mW. (c),(d) The theoretical fitting. (e) Measured forward (blue squares) and backward transmission (red dots) as a function of the pump field power. The lines are the theoretical fitting. The parameters for the theoretical curve are $\mu_{g_1,e_{11}} = 1.29 \times 10^{-29}$ C m, $\mu_{g_1,e_{12}} = 0.69 \times 10^{-29}$ C m, and $N = 2.5 \times 10^{17}$ m^{-3}.

As a further note, we not only achieve nonreciprocal transmission around $\delta_s/2\pi = 185$ MHz but in a broad operation bandwidth (more than $2\pi \times 100$ MHz), as demonstrated in Fig. 2(b). This is due to the existence of several hyperfine split energy levels [44]. For the D2 line of ^{85}Rb, $|5P_{3/2}, F = 1, 3\rangle$ are very close to $|5P_{3/2}, F = 2\rangle$. When the strong pump field is applied between $|5S_{1/2}, F = 2\rangle$ and $|5P_{3/2}, F = 2\rangle$ with a detuning of $2\pi \times 185$ MHz, it also acts as a strong pump field for the transition of $|5S_{1/2}, F = 2\rangle$ to $|5P_{3/2}, F = 1, 3\rangle$ with

the detuning of $2\pi \times 214$ and $2\pi \times 122$ MHz, respectively. But, because the transition of $|5P_{3/2}, F = 1\rangle$ to $|5S_{1/2}, F = 3\rangle$ is forbidden, the absorption and spontaneous emission cycle just happens for $|5P_{3/2}, F = 2, 3\rangle$. Therefore, two transmission peaks for the forward signal field around $2\pi \times 122$ and $2\pi \times 185$ MHz are present in our experiment. Since each of the two transmission peaks has a certain linewidth, they overlap partly and demonstrate a broad transmission bandwidth. For isolators, the realization of broadband is important in practice. We note that recently Xia *et al.* also proposed a theoretical scheme for broadband nonreciprocal transmission through chiral cross-Kerr nonlinearity with hot atoms [30]. The above single-signal-field experimental results are qualitatively well fitted by our theoretical results shown in Figs. 2(c) and 2(d) and the lines in Fig. 2(e) (the theoretical methods that we use are shown in Appendix A), thus fully confirming our physical insights and theoretical analysis.

Next, we perform the experiment with two signal fields. As shown in Fig. 3(a), the signal fields with 795 nm (3 μW) and 780 nm (3 μW) couple with the same ground state $|5S_{1/2}, F = 2\rangle$ and different excited states $|5P_{1/2}, F = 3\rangle$ and $|5P_{3/2}, F = 1, 2, 3\rangle$, respectively. The pump field keeps the power of 10 mW and detuning of $\delta_p/2\pi = 185$ MHz. The two transmitted signal fields are detected simultaneously by different detectors after being separated by a grating. Figures 3(b) and 3(c) demonstrate the recorded results that are plotted as functions of the signal detunings of $\delta_{s1} = \omega_{s1} - \omega_{g_1e_1}$ and $\delta_{s2} = \omega_{s2} - \omega_{g_1e_2}$, where $\omega_{g_1e_1}$ ($\omega_{g_1e_2}$) is the frequency difference between levels $|5S_{1/2}, F = 2\rangle$ and $|5P_{1/2}, F = 2\rangle$ ($|5P_{3/2}, F = 2\rangle$). A high transmission for the forward signal fields (dashed blue line) but nearly zero transmission for the backward signal fields (solid red line) at 795 and 780 nm is observed simultaneously. What needs to be emphasized here is that simultaneous realization of nonreciprocity for multiple signal fields is very important in multiwavelength optical systems such as WDM, and it is an essential difference between our scheme and the previous tunable wavelength schemes [32–35]. To characterize the optical isolation performance, we use the isolation ratio $\eta = 10|\log(T_f/T_b)|$ for evaluation [26]. Here, T_f and T_b are the transmission of the forward and backward signal fields. As shown in Figs. 3(b) and 3(c), the isolation ratios near 795 and 780 nm are about 25 and 28 dB, respectively, accompanied by a transmission higher than 0.85. Moreover, the operating range about a $2\pi \times 150$-MHz bandwidth with a transmission higher than 0.70 can be achieved at both wavelengths. Limited by our experimental conditions, we demonstrate here only two signal wavelengths at 795 and 780 nm. If lasers with other wavelengths are available, simultaneous nonreciprocal transmission for more wavelengths can be achieved.

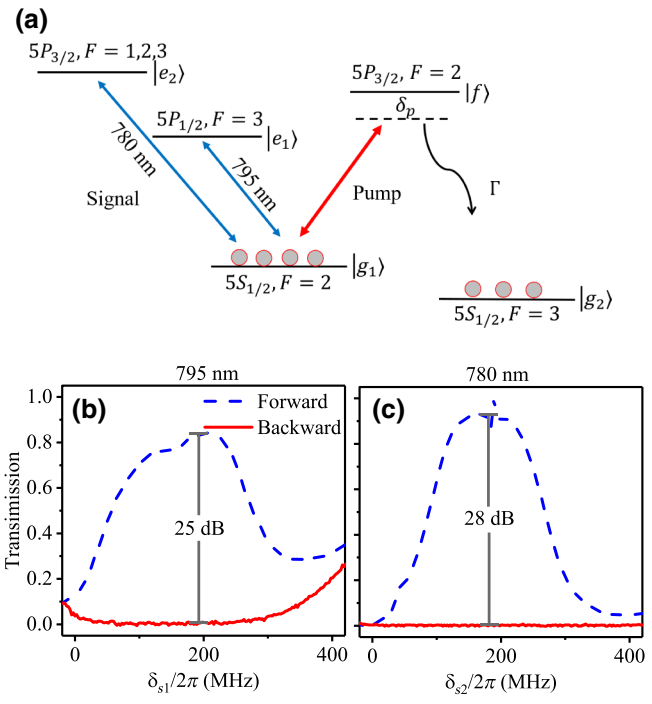

FIG. 3. (a) Multilevel V-type structure of ^{85}Rb atoms for two signal fields in isolation with a strong pump field. (b),(c) Simultaneous observation of normalized transmission for 795 and 780 nm. The pump field power is 10 mW and the signal field powers are 3 μW.

IV. CONCLUSION

In conclusion, we propose a scheme based on V-type warm atoms and an experimentally realized multiwavelength magnetic-free isolator by optical pumping. A nonreciprocal optical component that enables simultaneous isolation for multiple signal fields at different wavelengths is expected. This is shown by this work to be feasible via optical pumping with the assistance of the Doppler effect. We achieve more than a 25-dB isolation ratio with a transmission higher than 0.85 at 795 and 780 nm simultaneously using warm ^{85}Rb atomic ensemble. Furthermore, since the warm atoms can be uploaded into one-dimensional waveguides [45], our proposal may provide a feasible vision for miniaturized and integrated multiwavelength optical isolators.

ACKNOWLEDGMENTS

This work is supported by the National Natural Science Foundation of China (Grants No. 11874146, No. 11774089, and No. 11674094) and the Shanghai Natural Science Foundation (Grants No. 18DZ2252400, No. 17ZR1442700, and No. 18ZR1410500).

APPENDIX A: THEORETICAL MODEL

In order to better reflect the actual experimental results, when we perform the theoretical simulation, the hyperfine energy levels of the real atoms in the experiment are considered. The excited states $|f\rangle$ and $|e_i\rangle$ have multiple hyperfine levels. The pump field ω_p couples with the ground state $|g_1\rangle$ and excited states $|f_k\rangle$, where $|f_k\rangle$ represents the kth hyperfine level of state $|f\rangle$. The signal field ω_{si} couples with the ground state $|g_1\rangle$ and excited states $|e_{ij}\rangle$, where $|e_{ij}\rangle$ represents the jth hyperfine level of state $|e_i\rangle$ $(i,j,k = 1, 2, \ldots)$. The dynamics of the system is described by the following density matrix equation:

$$\dot{\rho} = -\frac{i}{\hbar}[H,\rho] + \dot{\rho}_{sp}, \tag{A1}$$

where ρ is the density operator and $\dot{\rho}_{sp}$ denotes the relaxation terms [46]. The total Hamiltonian H describing the multilevel atoms driven by the signal and the pump fields can be written as

$$H = \sum_k \hbar\Delta_{pk}|f_k\rangle\langle f_k| + \sum_{i,j}\hbar\Delta_{sij}|e_{ij}\rangle\langle e_{ij}| + \sum_k \hbar\Omega_{pk}|f_k\rangle\langle g_1| + \sum_{i,j}\hbar\Omega_{sij}|e_{ij}\rangle\langle g_1| + \text{H.c.}, \tag{A2}$$

where $\Delta_{pk} = \omega_p - \omega_{g_1 f_k} - k_p v$ and $\Delta_{sij} = \omega_{si} - \omega_{g_1 e_{ij}} \pm k_{si} v$ when we take the Doppler shift into account, $\omega_{g_1 f_k}$ $(\omega_{g_1 e_{ij}})$ is the frequency difference between levels $|g_1\rangle$ and $|f_k\rangle$ $(|e_{ij}\rangle)$, and Ω_{pk} (Ω_{sij}) is the Rabi frequency of the corresponding pump (signal) field.

Considering that all signal fields are weak, the linear susceptibility of the ith signal field, under the weak field approximation, can be written

$$\chi_i = \frac{N}{2\varepsilon_0\hbar}\int_{-\infty}^{\infty}\sum_j \frac{\mu_{g_1,e_{ij}}^2}{\Omega_{sij}}\langle e_{ij}|\rho^{(1)}|g_1\rangle D(v)dv, \tag{A3}$$

where N is the number of involved atoms, ε_0 is the permittivity of vacuum, $\mu_{g_1,e_{ij}}$ is the transition dipole moment between states $|g_1\rangle$ and $|e_{ij}\rangle$, and $\rho^{(1)}$ is the first-order solution of ρ. The velocity distribution $D(v) = \exp(-v^2/v_{mp}^2)/(\sqrt{\pi}v_{mp})$, where v_{mp} is the most probable velocity.

APPENDIX B: DETUNING OF THE PUMP FIELD

The detuning of the pump field is another tunable parameter in the system. Thus, we theoretically simulate the transmission of forward and backward signal fields as a function of δ_p. As shown in Fig. 4, when $\delta_p/2\pi$ is smaller than 160 MHz, the forward transmission is below 0.8.

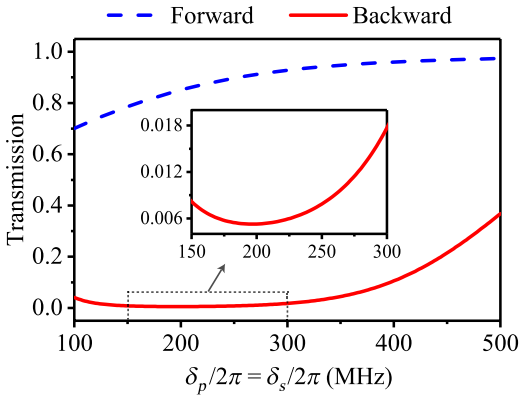

FIG. 4. Theoretical results for the forward and backward transmission versus δ_p, where $\delta_s = \delta_p$ and the pump field power is 10 mW. The other parameters are chosen to be the same as those in Fig. 2.

This is due to the existence of the hyperfine excited state $|5P_{1/2}, F = 2\rangle$, which causes a little absorption. Then with the increase of δ_p, the forward transmission increases and approaches to nearly 1. For the backward transmission, it remains almost zero near $\delta_s/2\pi = 200$ MHz and then increases gradually with δ_p. This relatively high backward transmission at larger δ_p stems from the reduction in the number of atoms. As is well known, the distribution of atomic number with velocity satisfies the Maxwell-Boltzmann distribution at room temperature. So, the number of atoms decreases with the velocity increasing. For larger δ_p, the atoms that can resonantly absorb the backward signal field become fewer, which leads to an increase in the backward transmission. As a result, the forward signal field has a high transmission over a wide range, and the backward one is well isolated around $\delta_s/2\pi = 200$ MHz (shown in Fig. 4). Therefore, we can choose $\delta_p/2\pi$ around 200 MHz to realize a relatively high-performance isolator. In our proof-of-concept experiment, the detuning of the pump field is selected to be $2\pi \times 185$ MHz.

[1] D. Jalas, A. Petrov, M. Eich, W. Freude, S. Fan, Z. Yu, R. Baets, M. Popović, A. Melloni, J. D. Joannopoulos, M. Vanwolleghem, C. R. Doerr, and H. Renner, What is – and what is not – an optical isolator, Nat. Photonics **7**, 579 (2013).

[2] C. Caloz, A. Alù, S. Tretyakov, D. Sounas, K. Achouri, and Z.-L. Deck-Léger, Electromagnetic Nonreciprocity, Phys. Rev. Appl. **10**, 047001 (2018).

[3] B. Peng, Ş. K. Özdemir, F. Lei, F. Monifi, M. Gianfreda, G. L. Long, S. Fan, F. Nori, C. M. Bender, and L. Yang, Parity–time-symmetric whispering-gallery microcavities, Nat. Phys. **10**, 394 (2014).

[4] L. Fan, J. Wang, L. T. Varghese, H. Shen, B. Niu, Y. Xuan, A. M. Weiner, and M. Qi, An all-silicon passive optical diode, Science **335**, 447 (2012).

[5] L. Chang, X. Jiang, S. Hua, C. Yang, J. Wen, L. Jiang, G. Wang, G. Li, and M. Xiao, Parity–time symmetry and variable optical isolation in active–passive-coupled microresonators, Nat. Photonics **8**, 524 (2014).

[6] N. Bender, S. Factor, J. D. Bodyfelt, H. Ramezani, D. N. Christodoulides, F. M. Ellis, and T. Kottos, Observation of Asymmetric Transport in Structures with Active Nonlinearities, Phys. Rev. Lett. **110**, 234101 (2013).

[7] D. L. Sounas, J. Soric, and A. Alù, Broadband passive isolators based on coupled nonlinear resonances, Nat. Electron. **1**, 113 (2018).

[8] L. Del Bino, J. M. Silver, M. T. M. Woodley, S. L. Stebbings, X. Zhao, and P. Del'Haye, Microresonator isolators and circulators based on the intrinsic nonreciprocity of the Kerr effect, Optica **5**, 279 (2018).

[9] D. L. Sounas and A. Alù, Non-reciprocal photonics based on time modulation, Nat. Photonics **11**, 774 (2017).

[10] Z. Yu and S. Fan, Complete optical isolation created by indirect interband photonic transitions, Nat. Photonics **3**, 91 (2009).

[11] D. L. Sounas and A. Alù, Angular-momentum-biased nanorings to realize magnetic-free integrated optical isolation, ACS Photonics **1**, 198 (2014).

[12] N. A. Estep, D. L. Sounas, J. Soric, and A. Alù, Magnetic-free non-reciprocity and isolation based on parametrically modulated coupled-resonator loops, Nat. Phys. **10**, 923 (2014).

[13] M. S. Kang, A. Butsch, and P. S. J. Russell, Reconfigurable light-driven opto-acoustic isolators in photonic crystal fibre, Nat. Photonics **5**, 549 (2011).

[14] K. Fang, J. Luo, A. Metelmann, M. H. Matheny, F. Marquardt, A. A. Clerk, and O. Painter, Generalized non-reciprocity in an optomechanical circuit via synthetic magnetism and reservoir engineering, Nat. Phys. **13**, 465 (2017).

[15] Z. Shen, Y.-L. Zhang, Y. Chen, C.-L. Zou, Y.-F. Xiao, X.-B. Zou, F.-W. Sun, G.-C. Guo, and C.-H. Dong, Experimental realization of optomechanically induced non-reciprocity, Nat. Photonics **10**, 657 (2016).

[16] Z. Shen, Y. L. Zhang, Y. Chen, F. W. Sun, X. B. Zou, G. C. Guo, C. L. Zou, and C. H. Dong, Reconfigurable optomechanical circulator and directional amplifier, Nat. Commun. **9**, 1797 (2018).

[17] F. Ruesink, M. A. Miri, A. Alù, and E. Verhagen, Nonreciprocity and magnetic-free isolation based on optomechanical interactions, Nat. Commun. **7**, 13662 (2016).

[18] F. Ruesink, J. P. Mathew, M. A. Miri, A. Alù, and E. Verhagen, Optical circulation in a multimode optomechanical resonator, Nat. Commun. **9**, 1798 (2018).

[19] H. Xu, L. Jiang, A. A. Clerk, and J. G. E. Harris, Nonreciprocal control and cooling of phonon modes in an optomechanical system, Nature **568**, 65 (2019).

[20] M.-A. Miri, F. Ruesink, E. Verhagen, and A. Alù, Optical Nonreciprocity Based on Optomechanical Coupling, Phys. Rev. Appl. **7**, 064014 (2017).

[21] S. Maayani, R. Dahan, Y. Kligerman, E. Moses, A. U. Hassan, H. Jing, F. Nori, D. N. Christodoulides, and T. Carmon, Flying couplers above spinning resonators generate irreversible refraction, Nature **558**, 569 (2018).

[22] D. W. Wang, H. T. Zhou, M. J. Guo, J. X. Zhang, J. Evers, and S. Y. Zhu, Optical Diode Made from a Moving Photonic Crystal, Phys. Rev. Lett. **110**, 093901 (2013).

[23] S. A. R. Horsley, J. H. Wu, M. Artoni, and G. C. La Rocca, Optical Nonreciprocity of Cold Atom Bragg Mirrors in Motion, Phys. Rev. Lett. **110**, 223602 (2013).

[24] P. Lodahl, S. Mahmoodian, S. Stobbe, A. Rauschenbeutel, P. Schneeweiss, J. Volz, H. Pichler, and P. Zoller, Chiral quantum optics, Nature **541**, 473 (2017).

[25] K. Xia, G. Lu, G. Lin, Y. Cheng, Y. Niu, S. Gong, and J. Twamley, Reversible nonmagnetic single-photon isolation using unbalanced quantum coupling, Phys. Rev. A **90**, 043802 (2014).

[26] C. Sayrin, C. Junge, R. Mitsch, B. Albrecht, D. O'Shea, P. Schneeweiss, J. Volz, and A. Rauschenbeutel, Nanophotonic Optical Isolator Controlled by the Internal State of Cold Atoms, Phys. Rev. X **5**, 041036 (2015).

[27] M. Scheucher, A. Hilico, E. Will, J. Volz, and A. Rauschenbeutel, Quantum optical circulator controlled by a single chirally coupled atom, Science **354**, 1577 (2016).

[28] I. Söllner, S. Mahmoodian, S. L. Hansen, L. Midolo, A. Javadi, G. Kiršanskė, T. Pregnolato, H. El-Ella, E. H. Lee, J. D. Song, S. Stobbe, and P. Lodahl, Deterministic photon-emitter coupling in chiral photonic circuits, Nat. Nanotechnol. **10**, 775 (2015).

[29] S. Zhang, Y. Hu, G. Lin, Y. Niu, K. Xia, J. Gong, and S. Gong, Thermal-motion-induced non-reciprocal quantum optical system, Nat. Photonics **12**, 744 (2018).

[30] K. Xia, F. Nori, and M. Xiao, Cavity-free Optical Isolators and Circulators Using a Chiral Cross-Kerr Nonlinearity, Phys. Rev. Lett. **121**, 203602 (2018).

[31] G. Lin, S. Zhang, Y. Hu, Y. Niu, J. Gong, and S. Gong, Nonreciprocal Amplification with Four-Level Hot Atoms, Phys. Rev. Lett. **123**, 033902 (2019).

[32] E. A. Kittlaus, N. T. Otterstrom, P. Kharel, S. Gertler, and P. T. Rakich, Non-reciprocal interband Brillouin modulation, Nat. Photonics **12**, 613 (2018).

[33] W.-B. Yan, W.-Y. Ni, J. Zhang, F.-Y. Zhang, and H. Fan, Tunable single-photon diode by chiral quantum physics, Phys. Rev. A **98**, 043852 (2018).

[34] C. Fan, F. Shi, H. Wu, and Y. Chen, Tunable all-optical plasmonic diode based on Fano resonance in nonlinear waveguide coupled with cavities, Opt. Lett. **40**, 2449 (2015).

[35] G. Li, X. Xiao, Y. Li, and X. Wang, Tunable optical nonreciprocity and a phonon-photon router in an optomechanical system with coupled mechanical and optical modes, Phys. Rev. A **97**, 023801 (2018).

[36] W. Happer, Optical pumping, Rev. Mod. Phys. **44**, 169 (1972).

[37] S. Chu, The manipulation of neutral particles, Rev. Mod. Phys. **70**, 685 (1998).

[38] C. N. Cohen-Tannoudji, Manipulating atoms with photons, Rev. Mod. Phys. **70**, 707 (1998).

[39] W. D. Phillips, Laser cooling and trapping of neutral atoms, Rev. Mod. Phys. **70**, 721 (1998).

[40] E. A. Cornell and C. E. Wieman, Nobel lecture: Bose-einstein condensation in a dilute gas, the first 70 years and some recent experiments, Rev. Mod. Phys. **74**, 875 (2002).

[41] W. Ketterle, Nobel lecture: When atoms behave as waves: Bose-Einstein condensation and the atom laser, Rev. Mod. Phys. **74**, 1131 (2002).

[42] W. Demtröder, *Laser Spectroscopy: Basic Concepts and Instrumentation* (Springer Science & Business Media, Berlin, 2013).

[43] M. D. Levenson and S. Kano, *Introduction to Nonlinear Laser Spectroscopy* (Academic Press, New York, 1988).

[44] D. Steck, Rubidium 85 D Line Data, http://steck.us/alkalidata.

[45] S. Ghosh, A. R. Bhagwat, C. K. Renshaw, S. Goh, A. L. Gaeta, and B. J. Kirby, Low-Light-Level Optical Interactions with Rubidium Vapor in a Photonic Band-Gap Fiber, Phys. Rev. Lett. **97**, 023603 (2006).

[46] M. O. Scully and M. S. Zubairy, *Quantum Optics* (Cambridge University Press, Cambridge, 1997).